

# CSC Electronics Performance Study at the beam.

Brookhaven National Laboratory

12 April 2000

## **Abstract**

The prototype of front-end electronics (amplifier and Switch Capacitance Array (SCA)) was tested with the CSC chamber on the beam at the X5 high radiation facility at CERN. The beam test demonstrated that the new electronics worked reliably at maximum background rate. The analysis of the beamtest data was dedicated the impact of the sampling readout on the CSC performance. The several amplitude finding algorithms was checked. The dependence the CSC resolution and efficiency on ADC precision was studied also. The comparison the previous analysis has showed that at the same condition the results are similar for both beamtest.

## **1 Experimental set-up**

During the October of 1999 the CSC prototype was tested at the X5 high radiation facility at CERN. The aim of this test was to get the first view at the prototypes of the front-end electronics (amplifiers and SCA). The CSC prototype and the Si telescope were the same as the previous beamtest-98. Fig.1 shows the layout of the beam test set-up. The Silicon microstrip telescope (Si) was installed at 1.5m from the CSC prototype and used to determine track parameters at the CSC position. The track position predicted by the Si telescope was used to measure CSC position resolution and track efficiency. Muon beam momentum was 80 GeV/c. Beam divergence at this momentum was 1.7 mrad. This enables to estimate the CSC resolution by comparison of the track

positions in two CSC layers with the precision good enough for quick on-line monitoring. The beam illuminated area of the chambers was determined by the  $5 \times 5 \text{ cm}^2$  trigger counters (Sc1, Sc2). The high intensity radioactive gamma source  $^{137}\text{Cs}$  was installed in the beam area. The variable lead absorbers were used to change the radiation flux intensity. The CSC prototype was placed at the distance of 1.5 m. from the gamma source. At this distance the open source provides the radiation background close to the one expected in the ATLAS at CSC position with the conventional safety factor 5 was taken into account.

The chamber parameters are following: anode-cathode spacing - 2.5 mm, anode wire diameter -  $30 \text{ }\mu\text{m}$ , the wire pitch - 2.5 mm, 20 anode wires join to one anode group, cathode strip readout pitch - 5 mm, this distance contains three equal strips, one of them is the readout and the other two are intermediate strips. In this test the gas composition was  $0.6\text{Ar} + 0.3\text{CO}_2 + 0.1\text{C}_2\text{H}_2\text{F}_4$ . The gas gain was about  $10^5$ .

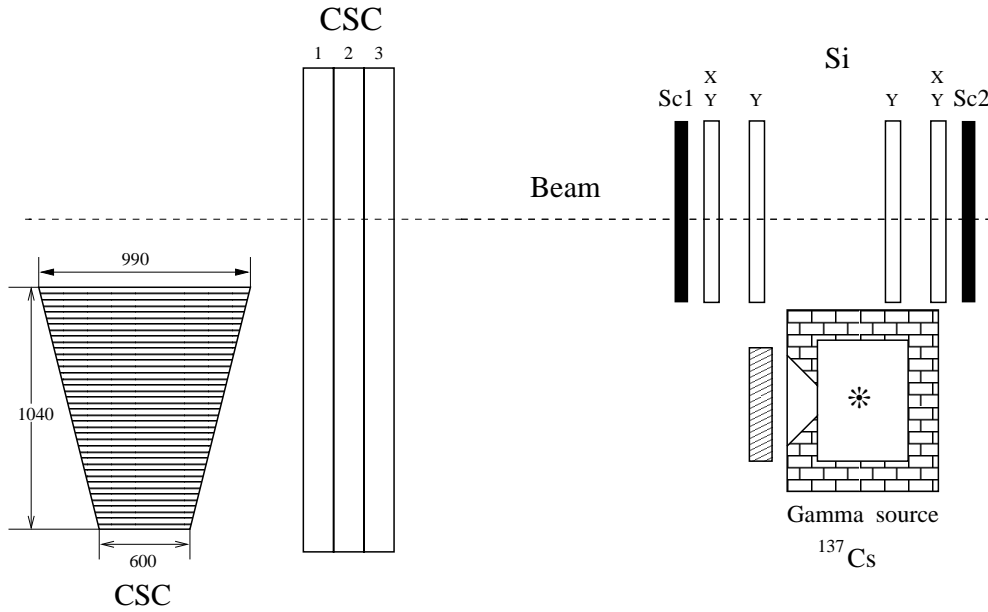


Figure 1: Beam test set-up layout.

Two kinds of amplifiers were used during this test. One CSC layer was equipped by prototype of the new amplifier chip, developed by BNL. The second plane was equipped by hybrid preamplifier and shaping amplifier of the old type. Signals from amplifiers were sampled, digitized and readed out by the Switch Capacitance Array (SCA). The SCA has a 14 bit ADC, 40 MHz write clock and

pine-line of 144 cells. Each trigger selected event was registered in 16 time samples with average signal maximum placed in ninth sample. The trigger was not synchronized with the SCA write clock, thus there was an additional 25 nsec uncertainty in the time position of the signal relative to the time samples. The own SCA noise was about five ADC counts. The shape of the amplifier signal was bipolar and the width of the positive part of the signal was 80 nsec (fwhm) for new amplifier and 120 nsec for the old one (fig.2). The curves on the fig.2 is the fit by the bipolar function:

$$f(z) = A \cdot \left(1 - \frac{z}{n+1}\right) \cdot z^n \cdot e^{-z}, \quad (1.1)$$

where  $n$  is a number of amplifier integration ( $n = 12$  for new amplifier and  $n = 6$  for old amplifier),  $z = (t-t_0)/\tau$ ,  $\tau$  is parameter reflected the width of the signal ( $fwhm = 1.28 \cdot \tau \cdot \sqrt{n+1}$ ),  $t_0$  is the start position of the signal.

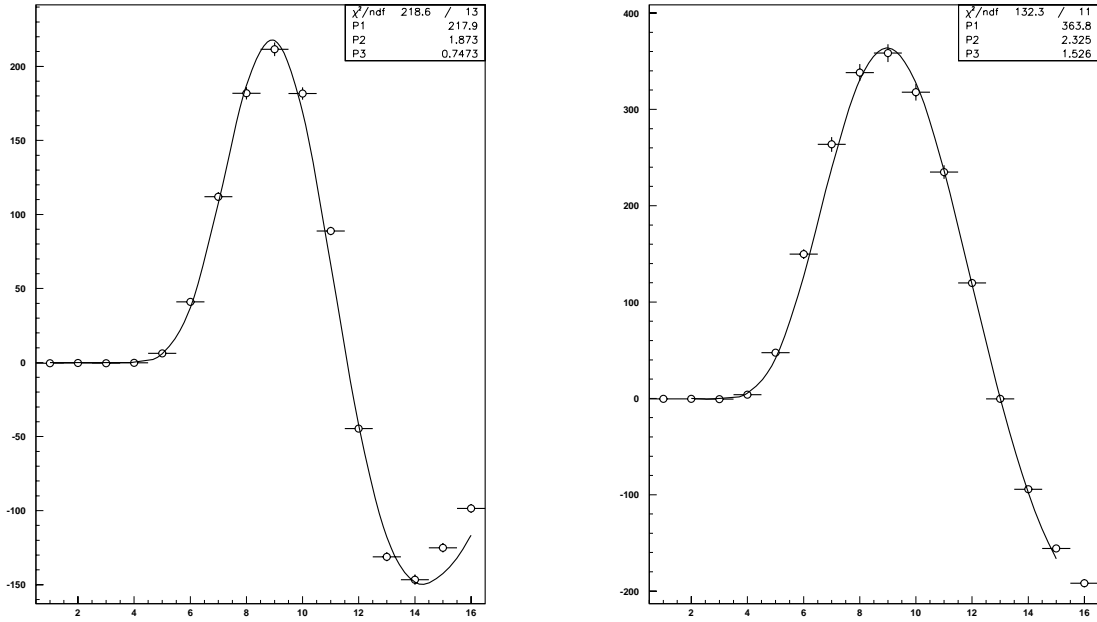


Figure 2: Measured average shape of signal from a) the new amplifier b) the old amplifier. The curves are the bipolar function fit.

The equivalent noise charge for both amplifiers was 3500 e. Perhaps, there was some contribution

to the noise from the environment. To unify the electronics gain of all channels the calibration was carried on regularly on a daily basis. For this purpose the amplitudes of the precision pulser were provided to one of the anode group and through the anode-cathode capacitances were provided for each cathode strips. This calibration was able to achieve the uniformity of the neighboring channels better than 0.5 percent. For each strip the average amplitude of the second sample from the same run was used as pedestal.

## 2 Data analysis and results

The detail study of the CSC performance at low rates has been done in our previous works [1,2]. The factors affected the high rate CSC performance was considered in the Atlas note [3]. Here we will consider new factors which arise from the registration shape of signal due to time sampling.

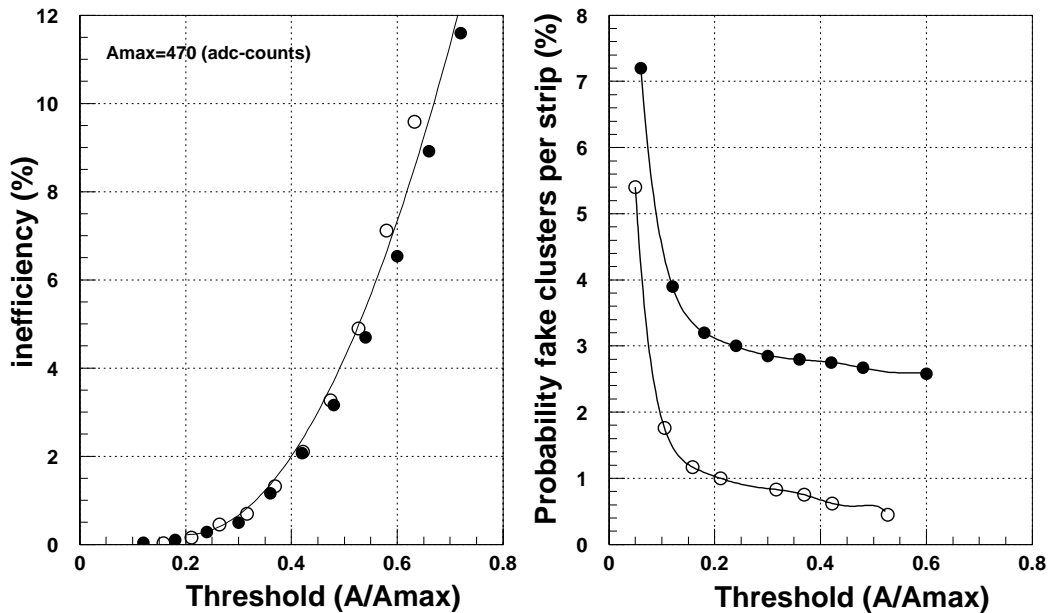


Figure 3: a) Cluster finding inefficiency versus threshold value. The threshold is normalized to Amax - most probable value of amplitude distribution in maximal strip. b) Probability of the fake hits per one strip versus threshold value.

The procedure of selection events for analysis was following. First of all, to select the perfect muon tracks some cuts were included: 1. all six Si planes should contain hits, 2. the track angle should be less  $\pm 2 mrad$ , 3. when the efficiency of one of the CSC layer was studied another layer must contained hit near the track ( $\pm 0.3 mm$ ). The next step was to find clusters in the chamber. The event information from one layer is divided by strips and samples into  $12 \times 16$  bins (12 strips and 16 t-samples). If the bin with a maximal amplitude was higher than the threshold, the event was selected for further analysis.

On the fig.3a a cluster inefficiency is shown versus the value of the threshold. For convenience, the threshold is normalized to the most probable amplitude of the charge deposited by the muon in the maximal strip. The fig.3b shows the probability to find a background fake cluster in one strip at maximal available in this beamtest rate  $1.9 kHz/cm^2$  (the maxialexpected LHC background rate at rapidity 2.7 is  $2.6 kHz/cm^2$ , if the factor safety five is taking into account).

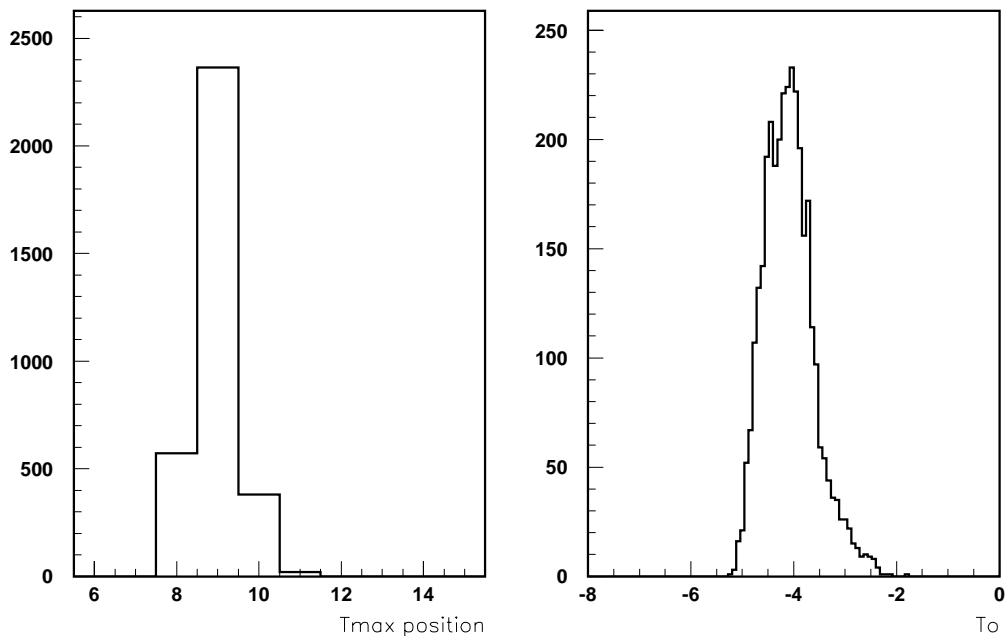


Figure 4: a) The maximal sample position. X axis in numbers of time sample. b) The time distribution of  $T_0$  (signal beginning time).

The one strip probability may be used to evaluate the number of fake clusters per one trigger and per one plane at the maximum expected LHC background rate. It can be seen from fig.3a,b that optimal threshold is 2.5, the probability to find a fake cluster at this threshold is 3%, the rapidity of the strip  $k$  is  $\eta_k = -\ln((r_0 + 0.5 \cdot k)/2L)$  ( $L$  is Z position first muon station,  $r_0$  is radial position of lowest strip), the dependence of the background rate per strip on rapidity is published in our Atlas note [3], so, joining all together, the total number of fake clusters in one plane per one trigger is equal 4.2.

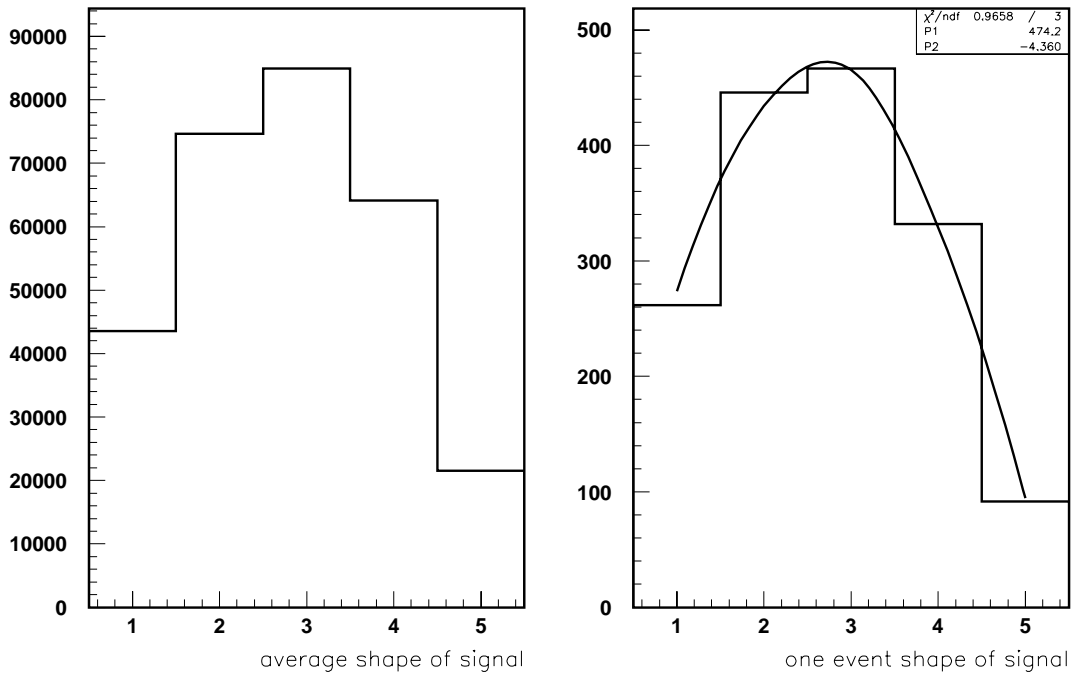


Figure 5: a) The average signal. b) The individual signal. The curve is the fit by bipolar function.

The amplitude finding algorithm is important to get a good position resolution. Indeed, even one percent amplitude uncertainty leads to an additional 50 micron contribution to the CSC position resolution. In previous tests we have used for the digitization a standard QDC or a pick sensitive ADC, in both cases the amplitude of the signal was defined by a hardware. In the case of SCA the signal time profile is registered instead, and the amplitude of the signal maximum should be defined by some algorithm. Potentially, this procedure may increase the error because the time position of

signal fluctuates due to the electron drift time and lack of synchronization of the SCA write clock and the muon trigger. The fig.4 shows the distributions of the arrival time of the maximal sample (fig.4a) and the time of beginning of signal T0 (fig.4b). The value of T0 was found from the fit of signal by bipolar function. It can be seen that the fluctuations of the signal position are significant. The probability to find the position of maximal sample farther than one sample from the average position is 0.6%

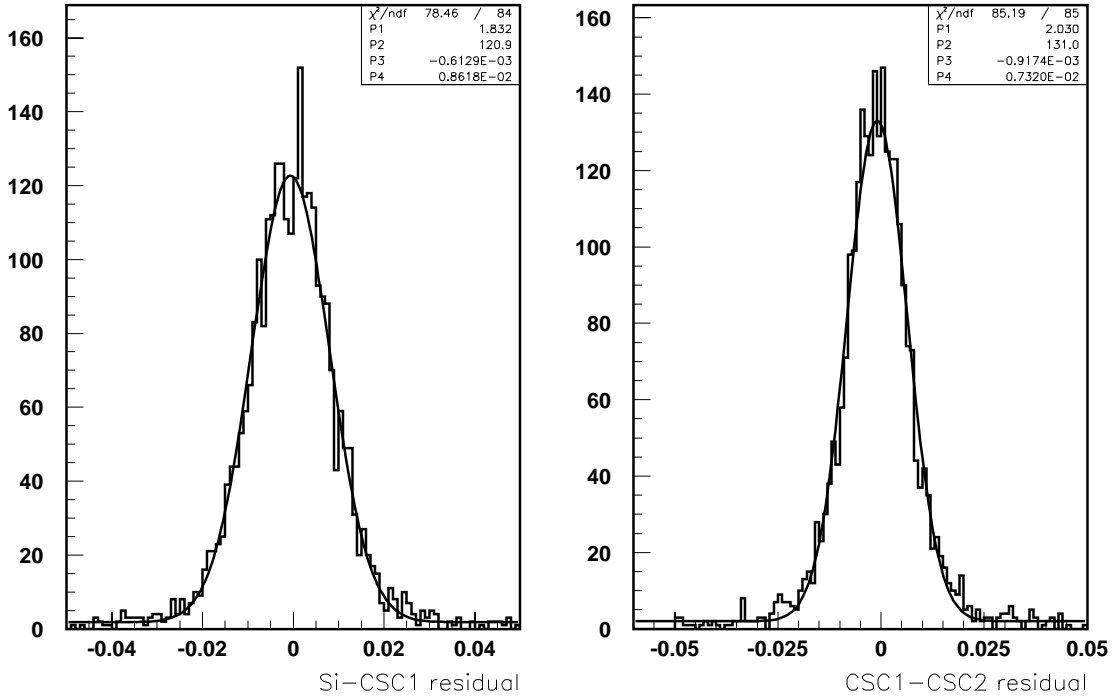


Figure 6: a) The Si-CSC1 residual. b) The CSC1-CSC2 residual. The curves are the fit by Gaussian plus constant.

In principle two approaches are possible to make up the amplitude finding algorithm. In one of them the maximum position is found at first and then some algorithm is applied in area around maximum to get the value of amplitude. This area may contain one or several samples. One of the examples of such an algorithm is the simple sum of the maximal sample and its nearest neighbors. In order for this algorithm to work properly, the gate should contain at least two samples more than the algorithm used. This is needed because the arriving time fluctuates and a narrow gate may be

reason losses some samples . In the second algorithm all samples are used no matter how signal places in the gate. Of course the reasonable result in this case may be got if the signal is fitted by some appropriate function.

Both amplitude finding algorithms were checked. In the first of them the maximum is found and then the maximal sample and its nearest neighbors are summed. We have studied the sum of 1,3 and 5 samples. The second algorithm fitted of signal by bipolar function and all sample inside gate were included in the fit. The bipolar function has four parameters. Two parameters ( $n$  and  $\tau$ ) were found by fitting the average signal shape and was then fixed. Another two ( $T_0$  and the amplitude) were determined from the fit of individual signals. This algorithm was checked for the gates contained 3,4,5 and 7 samples. On the fig.5 the example of the average and the individual signals are shown.

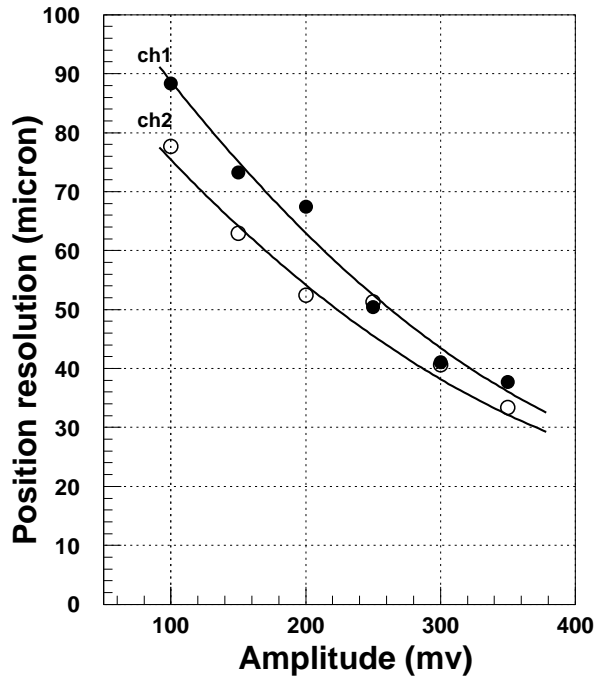


Figure 7: The dependence of the CSC position resolution on the amplitude . The solid and open points are CSC1 and CSC2 layers respectively.

After the amplitude was determined, the procedure of finding the cluster position was applied.



For this aim the maximum and its nearest neighbours from each side were selected and the cluster position was calculated by the ratio algorithm [3]. The fig.6a,b shows Si-CSC1 and CSC1-CSC2 residuals. Unfortunately, during this beamtest Si telescope resolution contributed to the residual significantly due to the multiple scattering of muons and large distance between Si and CSC. However we have three separate distribution (Si-CSC1, Si-CSC2 and CSC1-CSC2) and therefore are able to define all three values of position resolution. The resolution of Si telescope after extrapolation of the track to CSC position is equal 63 micron. The resolution CSC1 and CSC2 at low rate is 60 and 44 micron respectively.

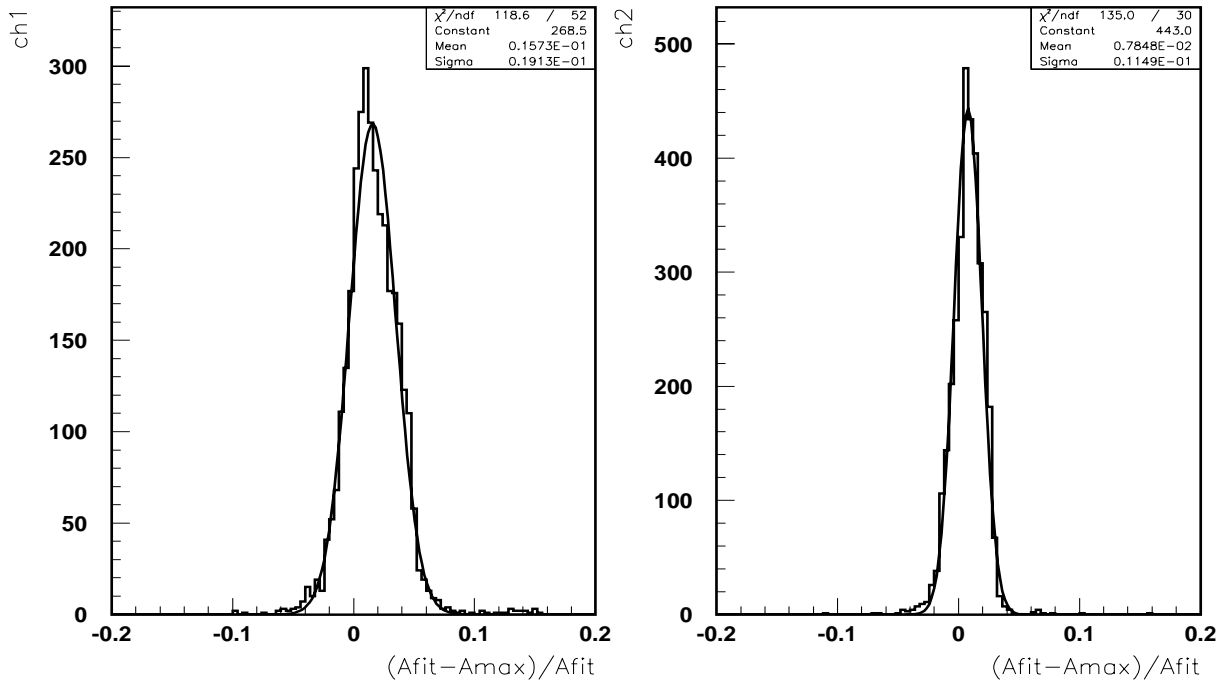


Figure 8: The relative difference of amplitudes found by fitting of signal ( $A_{fit}$ ) and maximal sample ( $A_{max}$ ). ( a) CSC1 and b) CSC2)

The reason of the difference of two CSC layers is mainly because of the difference of the gas gain in them. (gas gain of CSC2 was 1.5 time higher). If the resolution is compared at the same selected amplitudes the result is, practically, the same( see fig.7). The remaining difference can be explained by the fact that the amplitude finding algorithm is less precise for narrower CSC1 signals.

This clearly can be seen at fig.8 where the relative difference in amplitudes found from the fit and the maximal sample is shown for both layers. From this figure the difference in the second layer is significantly less (0.018 for CSC1 and 0.011 for CSC2).

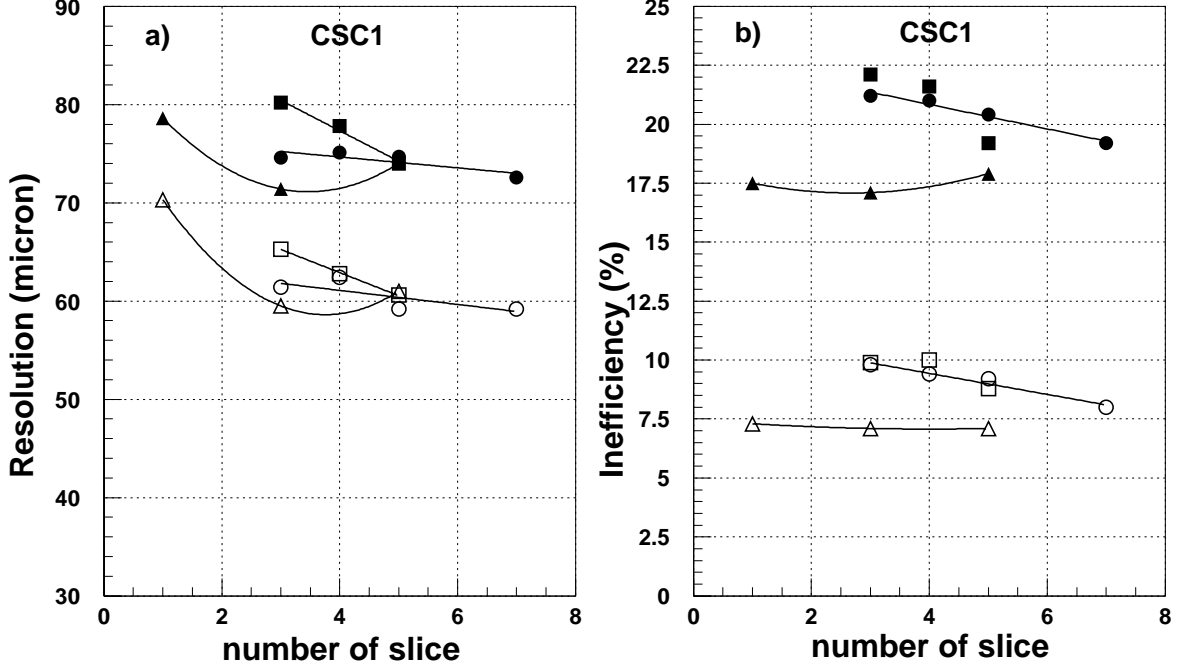


Figure 9: a) The CSC1 position resolution for different amplitude finding algorithms. The open and solid points are measured at low and high rates respectively. The triangles and circles present the sum and fitting algorithms respectively at 40MHz clock, the squares are the fitting algorithm at 20MHz clock. b) The CSC inefficiency for different amplitude finding algorithms at high and low background rates.

The fig.9a shows the dependence of the CSC1 position resolution and inefficiency on the number of samples involved in the amplitude finding algorithm. The squares and circles present the sum and the fitting algorithm respectively. The open and solid points present the measurement at low and high rates respectively. One may see that the sum algorithm has optimum at three involved samples. This is because on the one hand the amplitude is less sensitive to arriving signal time when more samples is added, on the other hand the noise accumulated with number of samples.

The CSC efficiency is defined as a fraction of events inside the fixed range of  $\pm 0.3mm$ . The total number of muons passed through the studied CSC chamber is defined by the Si telescope and another CSC layer. From fig.9 it can be seen that the sum algorithm gives slightly better results. However it is necessary to remember that two additional time samples should be written to realize this algorithm on the next level of analysis.

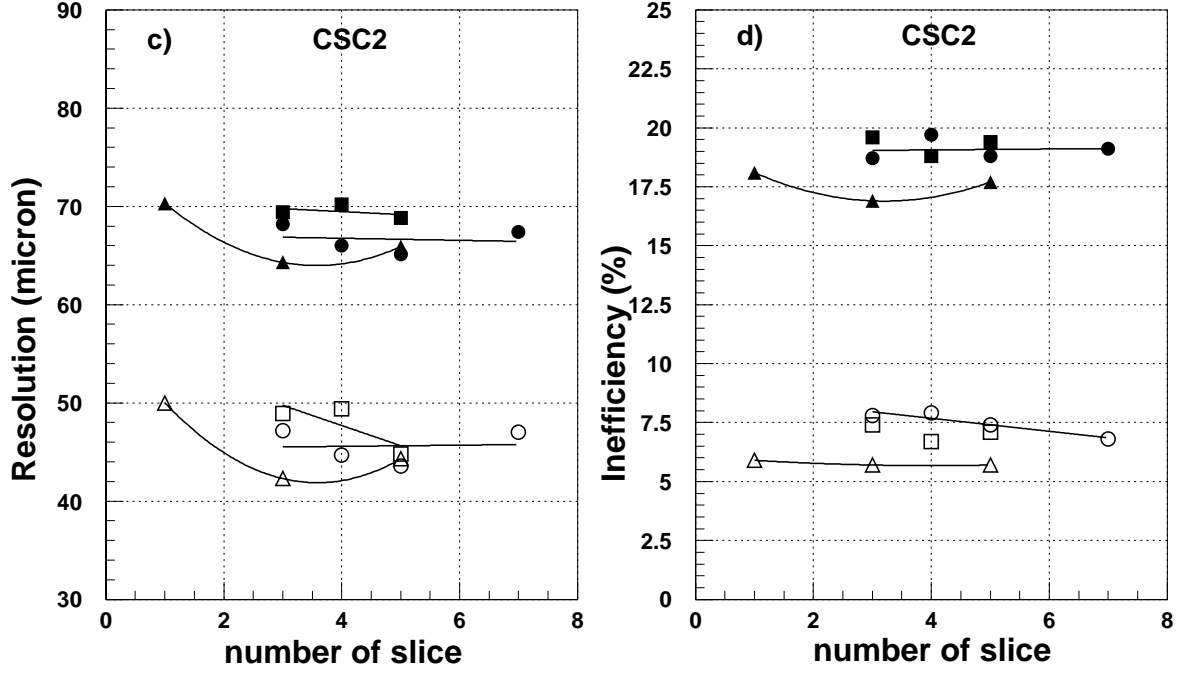


Figure 10: The CSC2 position resolution and inefficiency for different amplitude finding algorithms. The meaning of points the same as fig9.

The next question is how the dynamic range of readout electronics affects on the CSC efficiency. The distribution of amplitude from maximal strip is shown in fig.11a. In the given plot the dynamic range after pedestal subtraction was limited by 13 bits and amplitudes more than 13 bit accumulated in 8200 channel. It can be seen that the amplitude of signals has the wide distribution with a long tail and, practically, for any dynamic range the part of signals lays beyond the end of range. Thus this cause decreases the CSC efficiency. The fig.11b shows how CSC efficiency depends on the value of dynamic range. The dynamic range is normalized to the most probable

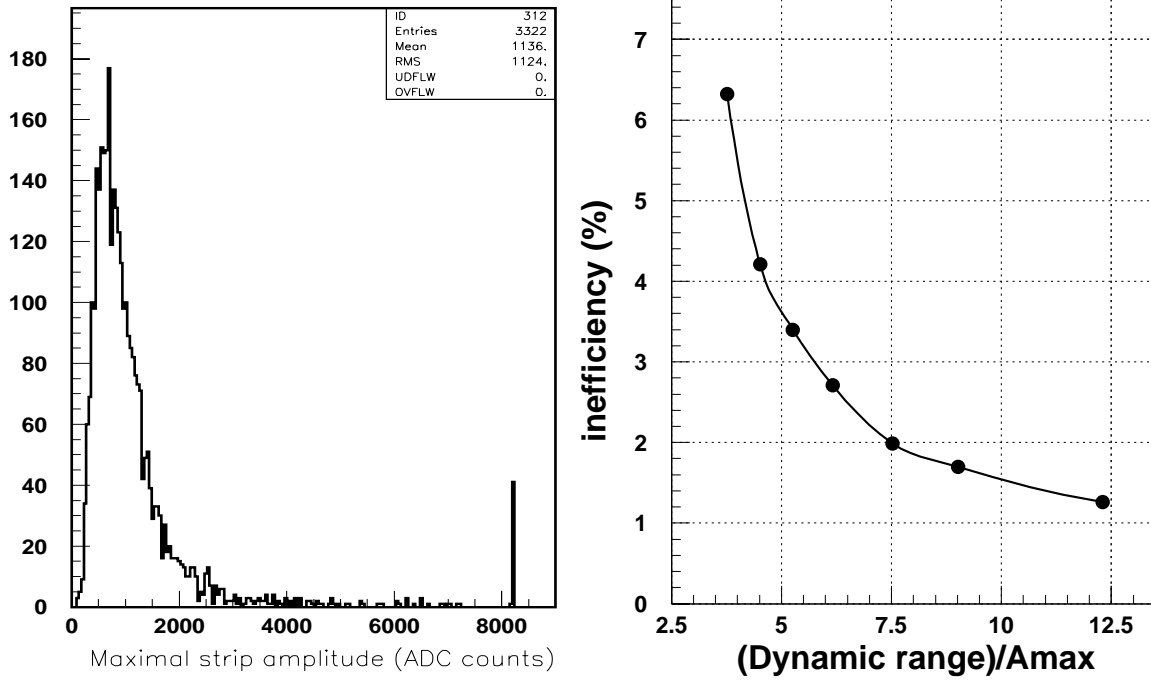


Figure 11: a) The maximal strip amplitude distribution. The dynamic range is 13 bits, the saturated signals are accumulated in the end of range b) the inefficiency versus the value of dynamic range. The range is normalized to the most probable amplitude deposited by muon in the maximal strip.

amplitude deposited by the muon in the maximal strip.

The digitization of the amplitude also may be the source of degradation CSC performance. In order to check how the ADC precision affects on the CSC resolution and efficiency we artistically varied number of K ADC bits when the amplitude was digitized. In this study the normalized dynamic range was fixed at the value 6.2 for all ADC precision. The fig.12 shows the dependences CSC resolution (fig.12a) and inefficiency (fig.12b) on the ADC precision. The open and solid points present low and high background rates respectively. The circle and square points present CSC1 and CSC2 layers. In this study five samples fitting algorithm was used to find amplitude and the ratio algorithm [3] to find the track position. It can be seen from fig.12 that the 10 bits ADC precision is enough in order the digitization contribution was negligible for both CSC resolution and efficiency.

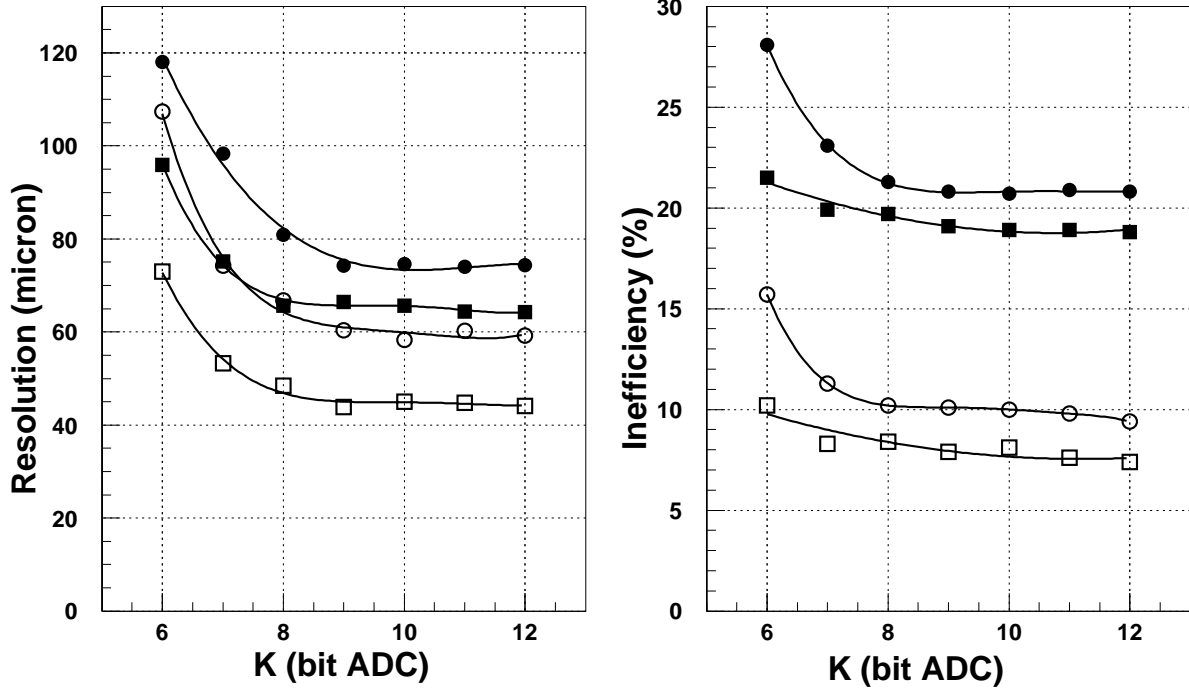


Figure 12: The CSC single plane a) position resolution and b) inefficiency versus the ADC precision. The solid and open points are data for low and high rate respectively. The circle and square points are CSC1 and CSC2 data respectively.

The dependence of the CSC position resolution (a) and inefficiency (b) on the background rate is presented in fig.13. To determine the amplitude of signal the algorithm the sum of three samples around maximum was applied. The solid and open points are data for CSC1 and CSC2 respectively, curves are beamtest-98 data. One can see that the behavior of the CSC performance with rate are similar for both beamtests.

### 3 Conclusion

During the beamtest the new front-end electronics showed the expected performance. The SCA time scanning readout requires new approach to get the signal amplitude. The CSC performance was checked for several amplitude finding algorithms. As the result it was shown that the four time

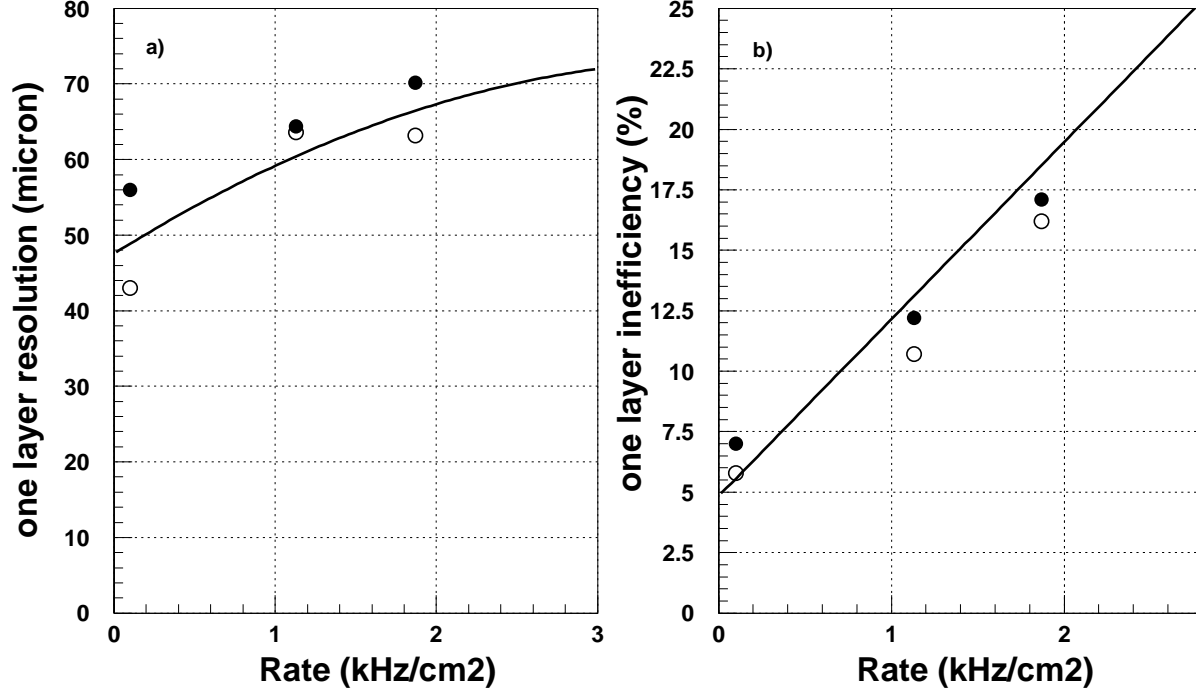


Figure 13: The CSC single plane a) position resolution and b) inefficiency versus the background rate. The solid and open points are data for CSC1 and CSC2 respectively. The curves are results of beamtest-98.

samples are enough to save parameters of signal for further analysis without any significant loss information. The best result showed algorithms which used area around maximal sample. However due to significant jitters of signal these algorithms require to write more samples for analysis than algorithms with fixed gate.

Also the dependence of the CSC performance on the ADC precision was studied and it has been shown that ADC precision should be not less than 9 bits in order to neglect this factor. The comparison the results of the previous beamtest analysis showed that at the same condition the results are very similar both for the CSC position resolution and for the CSC efficiency.

## 4 References

1. G.Bencze et al., Nucl.Instr. and Meth. A 357(1995) 40.
2. V.Gratchev et al., Nucl.Instr. and Meth. A 365(1995) 576.
3. A.Gordeev et al., Atlas note ATL-MUON-2000-005 (ATL-COM-MUON-99-032)